Materials Research. 2018; 21(4): e20180189
DOI: http://dx.doi.org/10.1590/1980-5373-MR-2018-0189

Experimental Study of the Tl_4PbTe_3-Tl_9TbTe_6-Tl_9BiTe_6 Section of the Tl-Pb-Bi-Tb-Te System

Samira Zakir Imamaliyeva[a]*, Ganira Ilgar Alakbarzade[b,c], Vagif Akber Gasymov[a], Mahammad Baba Babanly[a]

[a]Institute of Catalysis and Inorganic Chemistry, ANAS, Baku, Azerbaijan
[b]Azerbaijan State Oil and Industry University, Azadlig Ave., AZ-1010, Baku, Azerbaijan
[c]Azerbaijan National Aerospace Agency, Azadlig Ave., AZ-1106, Baku, Azerbaijan

Received: March 13, 2018; Revised: April 02, 2018; Accepted: April 20, 2018

The aim of the present study was to determine the phase relations in the Tl_4PbTe_3-Tl_9TbTe_6-Tl_9BiTe_6 section of the Tl-Pb-Bi-Tb-Te system. Based on a set of the methods of the physicochemical analysis (differential thermal analysis, powder X-ray diffraction method as well as microhardness measurements), the phase diagram of the Tl_4PbTe_3-Tl_9TbTe_6 boundary system, some isopleth sections, liquidus and solidus surfaces projections, as well as isothermal sections at 840 and 860 K, were plotted. Unlimited solid solutions with the Tl_5Te_3 structure (δ-phase) were found in the system, which are of interest as a thermoelectric materials.

Keywords: *thallium-lead telluride, thallium-terbium tellurides, thallium-bismuth tellurides, phase equilibria, liquidus and solidus surfaces, solid solutions.*

1. Introduction

Presently, great interest has devoted to the chalcogenides of heavy metals as prospective functional materials which found applications in the wide range of devices such as computer memories, chemical sensors, photo-detectors, solar cells, thermoelectric and optical devices, and ionic sensors[1-4]. Some of them expected as a good candidates for use in the spintronic devices[5,6]. The rare-earth materials, including chalcogenides, have been intensively investigated owing to their promising functional properties[7-11].

Tl_5Te_3 compound crystallizes in tetragonal structure (Sp. gr.I4/mcm, a = 8.930; c = 12.598 Å, z=4)[12,13]. The formula Tl_5Te_3 can thus be rewritten as $Tl_{16}[TlTe_3]_4$. The thallium atoms on the 4c site can be partially or fully replaced by other elements, resulting in a group of ternary compounds: $Tl_4A^{IV}Te_3$ and $Tl_9B^{V}Te_6$ -type (A^{IV}-Sn, Pb; B^{V}-Sb, Bi)[14-17]. Above-stated compounds possess a good thermoelectric performance[18-21] whereas Tl_9BiTe_6 found to have excellent thermoelectric properties with extremely low thermal conductivity at room temperature[18]. As it was shown by authors of the Ref.[21], the bulk superconductor Tl_5Te_3 and its tin-doped derivative $[Tl_4](Tl_{1-x}Sn_x)Te_3$ have Dirac-like surface states. Moreover, Tl_4SnS_3, Tl_4SnSe_3, Tl_4SnTe_3 compounds may be used for fabrication of IR induced electrooptically operated gratings[22].

New structural analogs of Tl_5Te_3 with common formula Tl_9LnTe_6 (Ln-Ce, Nd, Sm, Gd, Tb, Tm) were found in the[23,24]. Later, the crystal structure, thermoelectric and magnetic properties of a number Tl_9LnTe_6-type compounds were determined by H.Kleinke and co-workers[25,27].

The design and development of novel methods for controlled synthesis and growth of large single crystals require detailed studies of respective phase diagrams[28-30]. On the other hand, the improvement of thermoelectric performance can be achieved by introduction of the heavy metals into the crystal lattice[31]. With this aim, we presented the results of the study of phase relations for a number of systems including the Tl_5Te_3 compound and its structural analogs[32-35]. The formation of unlimited solid solutions was found for all these systems.

In this paper, we continued to study similar systems and presented the results of the study of the phase relations in the Tl_4PbTe_3-Tl_9TbTe_6-Tl_9BiTe_6 section of the Tl-Pb-Bi-Tb-Te system.

The initial compounds of above-mentioned system were studied in a number of papers. Tl_4PbTe_3 and Tl_9BiTe_6 melt congruently at 893 K[15] and 830 K[17] respectively, while Tl_9TbTe_6 is formed incongruently at 780 K[32]. The tetragonal lattice constants are following: a=8.841, c=13.056Å, z=4 (Tl_4PbTe_3)[36]; a=8.871; c=12.973 Å, z=2 Tl_9TbTe_6[33]; a = 8.855, c = 13.048 Å, z=2 (Tl_9BiTe_6)[37].

*e-mail: samira9597a@gmail.com

According to Ref.[38], the boundary system Tl_4PbTe_3-Tl_9BiTe_6 is quasi-binary and characterized by the formation of unlimited solid solutions (δ-phase) with Tl_5Te_3-structure.

Other boundary system Tl_9TbTe_6-Tl_9BiTe_6 was shown to contain a continuous series of solid solutions with a Tl_5Te_3 tetragonal structure, but not quasi-binary due to the incongruent melting of Tl_9TbTe_6 compound[32].

2. Experimental

2.1. Materials and syntheses

The ternaries synthesized from the high purity elements (Tl-99.999%, Pb-99.99%, Tb-99.9%, Bi-99.999%, Te-99.999%).

All synthesis were carried out in previously cleaned and dried quartz ampoules. Taking into account the high toxicity of thallium and its compounds, we used protective gloves at all times when working.

Stoichiometric amounts of the starting components were put into silica tubes of about 20 cm in length and diameter of about 1.5 cm and sealed under a pressure of 10^{-2} Pa. Tl_4PbTe_3 and Tl_9BiTe_6 were synthesized by direct synthesis of elemental components in a resistance furnace at 920 K followed by cooling in the switched-off furnace.

The synthesis of Tl_9TbTe_6 was carried out at 1000 K in the graphitized ampoule in order to avoid the interaction between the terbium and quartz. Then the intermediate ingot of Tl_9TbTe_6 was powdered in an agate mortar, thoroughly mixed, pressed into a pellet and annealed at 750 K during ~700 h.

The ampoules were shaken during all the heating process in order to help the complete mixing of all the elements.

We used the differential thermal analysis (DTA) and X-ray diffraction (XRD) in order to control the purity of synthesized compounds. Only one thermal effect was observed for Tl_9BiTe_6 (830 K) and Tl_4PbTe_3 (893 K), while two peaks for Tl_9TbTe_6 compound which are relevant to the peritectic reaction at 780 K and its liquidus at 1110 K. These data agree with the literature data[13,17,33]. The X-ray patterns showed that the desired compounds Tl_4PbTe_3, Tl_9TbTe_6 and Tl_9BiTe_6 formed as pure phases.

The multicomponent alloys of the Tl_4PbTe_3-Tl_9TbTe_6-Tl_9BiTe_6 section were prepared by melting of previously synthesized ternary compounds. After thermal treatment at 1000 K for 24-36 h, the samples were slowly cooled (20-30 K per hour) down to 750 K and annealed within 1000 h in order to complete the homogenization.

2.2. Methods

We used the DTA and XRD methods, as well as microhardness measurements to analyze the samples of the Tl_4PbTe_3-Tl_9TbTe_6-Tl_9BiTe_6 section.

The temperatures of the thermal effects were determined using a NETZSCH 404 F1 Pegasus differential scanning calorimeter within room temperature and ~1400 K at a heating rate of 10 $K.min^{-1}$ and accuracy of ±2 K. The phase composition of the powdered samples was identified by powder X-ray diffraction Bruker D8 diffractometer with CuK_α radiation within $10° \leq 2\theta \leq 70°$ at room temperature. The unit cell parameters of intermediate alloys were calculated by indexing of powder patterns using Topas V3.0 software. An accuracy of the crystal lattice parameters is shown in parentheses (Table 1). Microhardness measurements were done with a microhardness tester PMT-3, the typical loading being 20 g and accuracy about 20 MPa.

3. Results and Discussion

The character of the phase relations along the Tl_4PbTe_3-Tl_9TbTe_6-Tl_9BiTe_6 section is established based on combined analysis of experimental results and literature data on boundary systems Tl_4PbTe_3-Tl_9BiTe_6[38] and Tl_9TbTe_6-Tl_9BiTe_6[33] (Fig.1-6).

3.1. Tl_4PbTe_3-Tl_9TbTe_6 boundary section

The results of DTA, XRD and microhardness measurements for starting compounds and some intermediate alloys of the Tl_4PbTe_3-Tl_9TbTe_6 section are presented in Table 1. This section (Fig.1) is characterized by the formation of

Table 1. Dependence of the properties of the alloys annealed at the 750 K (1000 h) on the composition for the Tl_4PbTe_3-Tl_9TbTe_6 section of the Tl-Pb-Bi-Tb-Te system

Solid phase compositions	Thermal effects, K	Microhardness, MPa	Tetragonal lattice parameters, Å	
			a	***c***
Tl_4PbTe_3	893	1120	8.8409(9)	13.0556(12)
$Tl_{8.2}Pb_{1.6}Tb_{0.2}Te_6$	860-885	1145	8.8470(8)	13.0390(11)
$Tl_{8.4}Pb_{1.2}Tb_{0.4}Te_6$	835-865	1155	8.8530(7)	13.0226(10)
$Tl_{8.5}Pb_{1.0}Tb_{0.5}Te_6$	825-853	-	-	-
$Tl_{8.6}Pb_{0.8}Tb_{0.6}Te_6$	815-845	1145	8.8590(8)	13.0060(10)
$Tl_{8.8}Pb_{0.4}Tb_{0.8}Te_6$	800-815; 1030	1125	8.8650(9)	12.9895(12)
$Tl_{8.9}Pb_{0.2}Tb_{0.9}Te_6$	790-800; 1080	-	-	-
Tl_9TbTe_6	780; 1110	1100	8.871(10)	12.9730(14)

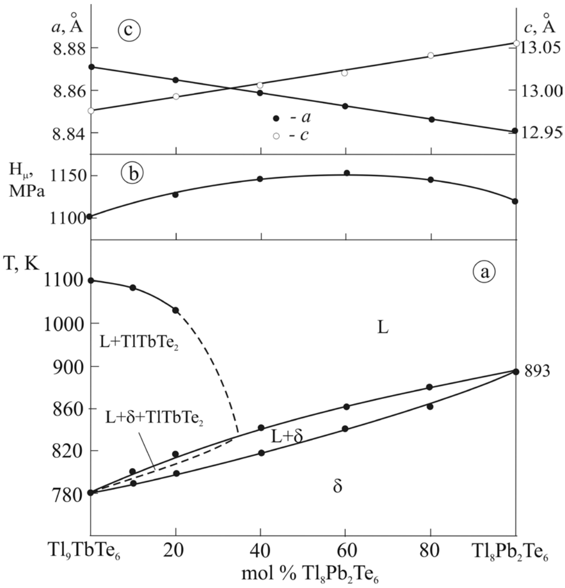

Figure 1. Phase diagram (a), concentration dependencies of microhardness (b), and lattice parameters (c) for the alloys of the Tl_9TbTe_6-$2Tl_4PbTe_3$ section.

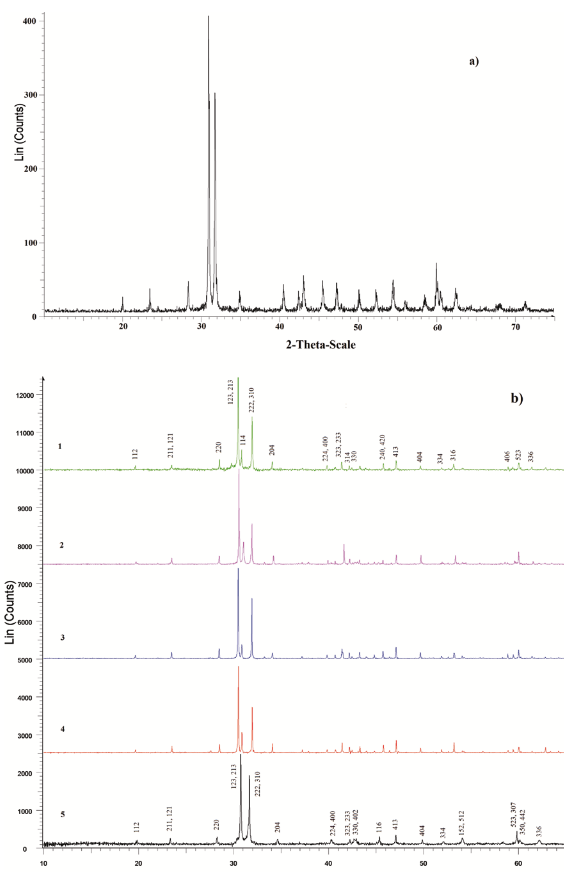

Figure 2. XRD powder patterns for Tl_5Te_3 (a), as well as Tl_4PbTe_3, Tl_9TbTe_6 and some alloys of the Tl_4PbTe_3-Tl_9TbTe_6 section (b). 1- Tl_4PbTe_3; 2-20 mol% Tl_9TbTe_6;3-50 mol% Tl_9TbTe_6; 4-80 mol% Tl_9TbTe_6; 5-Tl_9TbTe_6.

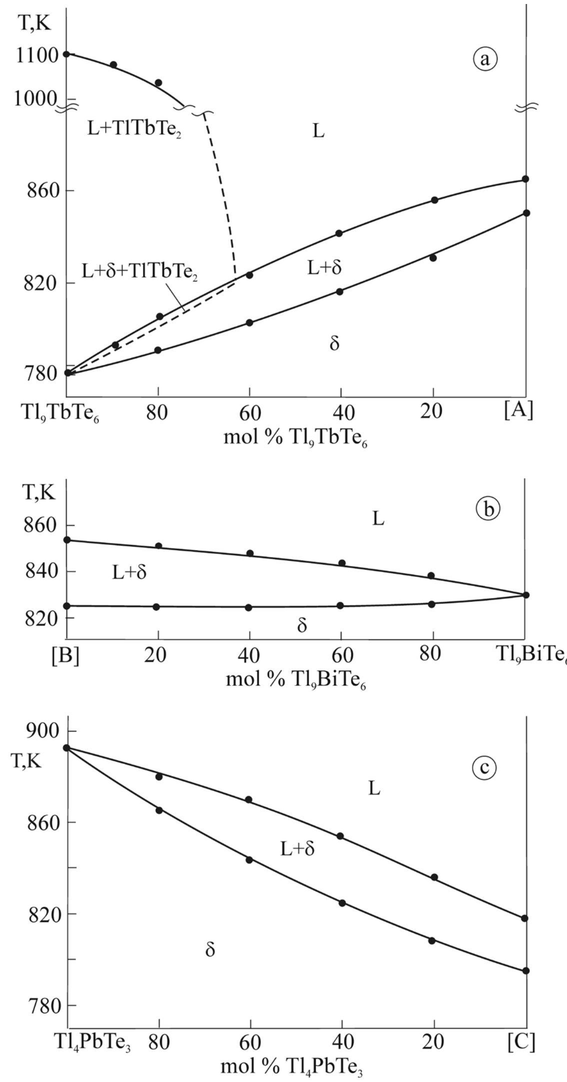

Figure 3. Polythermal sections Tl_9TbTe_6-[A], Tl_9BiTe_6-[B] and Tl_4PbTe_3-[C] of the Tl_4PbTe_3-Tl_9TbTe_6-Tl_9BiTe_6 concentration area of the phase diagram of the Tl-Pb-Bi-Tb-Te system. A, B, and C are equimolar alloys from the respective boundary system as shown in Fig.4.

unlimited solid solutions (δ-phase) with Tl_5Te_3-structure. However, it is a non-quasi-binary section of the Tl-Pb-Tb-Te quaternary system due to the peritectic character of melting of the Tl_9TbTe_6 compound. This leads to the crystallization of $TlTbTe_2$ compound in a wide composition interval and to the formation of L+$TlTbTe_2$ two-phase and L+$TlTbTe_2$+δ three-phase areas. Due to a narrow interval of temperatures, the area L+$TlTbTe_2$+δ is not fixed experimentally and shown by a dashed line.

The dependences of microhardness on composition have a flat maximum which is typical for systems with unlimited solid solutions (Fig.1b)[39].

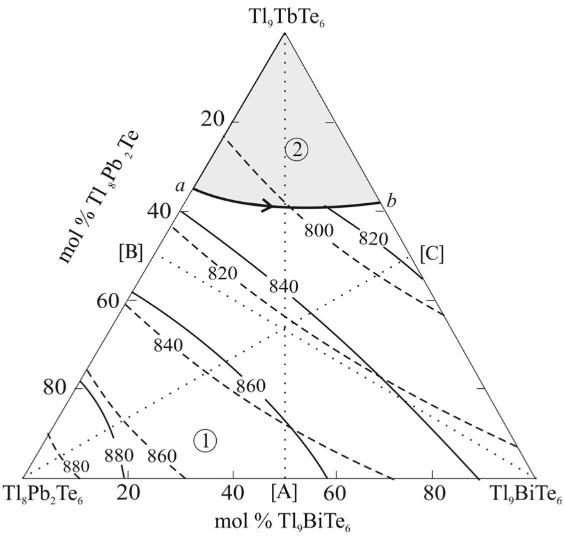

Figure 4. The liquidus and solidus surfaces projections Tl_4PbTe_3-Tl_9TbTe_6-Tl_9BiTe_6 section of the Tl-Pb-Bi-Tb-Te system. The investigated polythermal sections are shown by dash-dot lines. A, B and C are equimolar compositions of the boundary systems. Primary crystallization phases: 1-δ; 2-$TlTbTe_2$.

The XRD powder patterns for some alloys of the Tl_4PbTe_3-Tl_9TbTe_6 section as well as Tl_5Te_3 are presented in Fig.2. Powder diffraction patterns of Tl_4PbTe_3, Tl_9TbTe_6 and also intermediate alloys are single-phase and have the diffraction patterns qualitatively similar to Tl_5Te_3 with slight reflections displacement from one compound to another. For example, we present the powder diffraction patterns of alloys with composition 20, 50 and 80 mol% Tl_9TbTe_6. Parameters of the tetragonal lattice of solid solutions obey the Vegard's law (Table 1, Fig.1c)[40].

3.2. Isopleth sections of the phase diagram

We plotted some isopleth sections, in order to construct a complete T-x-y diagram. Figs.3a-c present the isopleth sections Tl_9TbTe_6-[A], Tl_9BiTe_6-[B] and Tl_4PbTe_3-[C] of the Tl_4PbTe_3-Tl_9TbTe_6-Tl_9BiTe_6 concentrations area, where A, B, and C are equimolar alloys from the respective boundary system as shown in Fig.4.

According to Fig.3a, b, the Tl_4PbTe_3-[C] and Tl_9BiTe_6-[B] sections are characterized by primary crystallization of the δ-phase from the melt over the entire concentration interval.

In contrast to the above-mentioned sections, along the Tl_9TbTe_6-[A] section, the direct crystallization of the δ-phase from the melt occurs only in the interval <60 mol% Tl_9TbTe_6. In the Tl_9TbTe_6-rich concentration area, the more refractory phase of $TlTbTe_2$ first crystallizes from the melt. Then a monovariant peritectic process L+TlTbTe↔δ occurs (Fig.3c), as a result of which a three-phase region L+$TlTbTe_2$+δ should form on the phase diagram. However, according to DTA data, we were unable to fix this region, which is apparently associated with the narrowness of the temperature interval of the above-stated peritectic reaction. Therefore, this region is indicated by the dotted line (Fig. 3b). The crystallization of all alloys is completed by the formation of δ-phase. The $TlTbTe_2$ phase is completely consumed in the peritectic reaction L+$TlTbTe_2$↔δ, and the remaining excess of the melt crystallizes into the δ-phase.

The XRD powder patterns for selective alloys on polythermal sections confirmed the formation of continuous solid solutions with the Tl_5Te_3-structure.

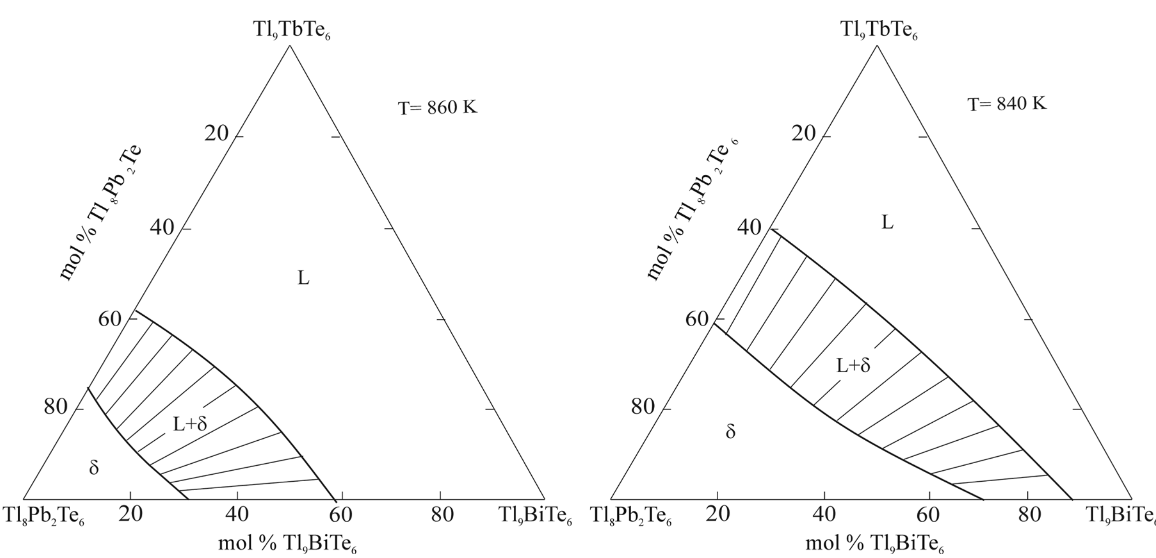

Figure 5. Isothermal sections at 860 and 840 K in the Tl_4PbTe_3-Tl_9Tb_6-Tl_9BiTe_6 section of the Tl-Pb-Bi-Tb-Te system.

3.3. The liquidus and solidus surfaces projections

Projection of liquidus of the Tl_4PbTe_3-Tl_9TbTe_6-Tl_9BiTe_6 section consists of two fields of the primary crystallization of $TlTbTe_2$ and δ- solid solutions. These fields are separated by a monovariant peritectic curve L+$TlTbTe_2$↔δ (ab curve). The solidus projection (dashed lines) consist of one surface corresponding to the completion of the crystallization of the δ-phase.

3.4. Isothermal sections at 860 and 840 K

Both sections are consist of areas of L-, $TlTbTe_2$ and δ-phases (Fig.5). In alloys with composition <60 mol% Tl_9TbTe_6 in the two-phase L+δ region the directions of the tie-lines on the studied composition plane. It should be noted that comparison of the isopleth sections (Fig.3) and isothermal sections (Fig.5) shows that the directions of the connodes in the two-phase region L+δ deviate from the *T-x* plane and constantly vary with temperature. Isothermal sections at 860 and 840 K clearly confirm this.

4. Conclusion

At the first time, a self-consistent scheme of the phase relations in the Tl_4PbTe_3-Tl_9TbTe_6-Tl_9BiTe_6 section of the Tl-Pb-Bi-Tb-Te system is obtained. The T-x diagrams of boundary system Tl_4PbTe_3-Tl_9TbTe_6, some isopleth sections, an isothermal section at 860 and 840 K, as well as liquidus and solidus surface projections, are plotted. It was shown, that studied system is characterized by the formation of the continuous field of δ-solid solutions with the Tl_5Te_3 structure. Obtained experimental results can be used for choosing the composition of solution-melt for the growth of the high-quality crystals of δ-phase which are of interest as thermoelectric materials.

5. Acknowledgment

The work has been carried out within the framework of the international joint research laboratory "Advanced Materials for Spintronics and Quantum Computing" (AMSQC) established between Institute of Catalysis and Inorganic Chemistry of ANAS (Azerbaijan) and Donostia International Physics Center (Basque Country, Spain).

6. References

1. Ahluwalia GK, ed. *Applications of Chalcogenides: S, Se, and Te*. New York: Springer; 2016.
2. Kolobov AV, Tominaga J. *Chalcogenides. Metastability and Phase Change Phenomena*. New York: Springer; 2012.
3. Shevelkov AV. Chemical aspects of thermoelectric materials engineering. *Russian Chemical Reviews*. 2008;77(1):1-20.
4. Cheng L, Li D, Dong X, Ma Q, Yu W, Wang X, et al. Synthesis, Characterization and Photocatalytic Performance of SnS Nanofibers and SnSe Nanofibers Derived from the Electrospinning-made SnO_2 Nanofibers. *Materials Research*. 2017;20(6):1748-1755.
5. Papagno M, Eremeev S, Fujii J, Aliev ZS, Babanly MB, Mahatha SK, et al. Multiple Coexisting Dirac Surface States in Three-Dimensional Topological Insulator $PbBi_6Te_{10}$. *ACS Nano*. 2016;10(3):3518-3524.
6. Caputo M, Panighel M, Lisi S, Khali L, DiSanto G, Papalazarou E, et al. Manipulating the Topological Interface by Molecular Adsorbates: Adsorption of Co-Phthalocyanine on Bi_2Se_3. *Nano Letters*. 2016;16(6):3409-3414.
7. Jha AR. *Rare Earth Materials: Properties and Applications*. Boca Raton: CRC Press; 2014.
8. Yaprintsev YM, Lyubushkin R, Soklakova O, Ivanov O. Effects of Lu and Tm Doping on Thermoelectric Properties of Bi_2Te_3 Compound. *Journal of Electronic Materials*. 2018;47(2):1362-1370.
9. Han F, Liu H, Malliakas CD, Sturza M, Wan X, Kanatzidis MG. $La_{1-x}Bi_{1+x}S_3$ (x ≈ 0.08): An n-Type Semiconductor. *Inorganic Chemistry*. 2016;55(7):3547-3552.
10. Alemi A, Klein A, Meyer G, Dolatyari M, Babalou A. Synthesis of New $Ln_xBi_{2-x}Se_3$ (Ln: Sm^{3+}, Eu^{3+}, Gd^{3+}, Tb^{3+}) Nanomaterials and Investigation of Their Optical Properties. *Zeitschrift für anorganische und allgemeine Chemie*. 2011;637(1):87-93.
11. Bao L, Zhang Z, Le Q, Li Q, Cui G. Influence of Gd, Nd and Ce Additions on Microstructures and Mechanical Properties of Ultra-light Dual Phase Mg-9Li-0.4Zr Alloys. *Materials Research*. 2016;19(3):654-658.
12. Schewe I, Böttcher P, von Schnering HG. The crystal structure of Tl_5Te_3 and its relationship to the Cr_5B_3 type. *Zeitschrift für Kristallographie*. 1989;188(1-4):287-298.
13. Černý R, Joubert J, Filinchuk Y, Feutelais Y. Tl_2Te and its relationship with Tl_5Te_3. *Acta Crystallographica C*. 2002;58(5):63-65.
14. Gotuk AA, Babanly MB, Kuliev AA. Phase equilibria in the Tl-Sn-Te system. *Neorganic Materials*. 1979;15(8):1356-1361.
15. Gotuk AA, Babanly MB, Kuliev AA. Phase equilibria in the systems Tl_2Te-SnTe and Tl_2Te-PbTe. *Uch. Zap. Azerb. Gos. Univ. Ser. Khim*. 1978;(3):50-56.
16. Babanly MB, Azizulla A, Kuliev AA. System Tl-Sb-Te. *Russian Journal of Inorganic Chemistry*. 1985;30:1051-1059.
17. Babanly MB, Akhmadyar A, Kuliev AA. System Tl_2Te-Bi_2Te_3-Te. *Russian Journal of Inorganic Chemistry*. 1985;30(9):2356-2359.
18. Wölfing B, Kloc C, Teubner J, Bucher E. High performance thermoelectric Tl_9BiTe_6 with an extremely low thermal conductivity. *Physical Review Letters*. 2001;86(19):4350-4353.
19. Guo Q, Chan M, Kuropatwa BA, Kleinke H. Enhanced Thermoelectric Properties of Variants of Tl_9SbTe_6 and Tl_9BiTe_6. *Chemistry of Materials.* 2013;25(20):4097-4104.
20. Kosuga A, Kurosaki K, Muta H, Yamanaka S. Thermoelectric properties of Tl-X-Te (X = Ge, Sn, and Pb) compounds with low lattice thermal conductivity. *Journal of Applied Physics*. 2006;99(6):063705.

21. Arpino KE, Wallace DC, Nie YF, Birol T, King PDC, Chatterjee S, et al. Evidence for Topologically Protected Surface States and a Superconducting Phase in $[Tl_4](Tl_{1-x}Sn_x)Te_3$ Using Photoemission, Specific Heat, and Magnetization Measurements, and Density Functional Theory. *Physical Review Letters*. 2014;112(1):017002.

22. Barchij I, Sabov M, El-Naggar AM, Al Zayed NS, Albassam AA, Fedorchuket AO, et al. Tl_4SnS_3, Tl_4SnSe_3 and Tl_4SnTe_3 crystals as novel IR induced optoelectronic materials. *Journal Materials Science: Materials in Electronics*. 2016;27(4):3901-3905.

23. Imamalieva SZ, Sadygov FM, Babanly MB. New thallium - neodymium tellurides. *Inorganic Materials*. 2008;44(9):935-938.

24. Babanly MB, Imamalieva SZ, Babanly DM. Tl_9LnTe_6 (Ln-Ce, Sm, Gd) compounds - the new structural analogies of Tl_5Te_3. *Azerbaijan Chemical Journal*. 2009;2:122-125. (In Russian).

25. Bangarigadu-Sanasy S, Sankar CR, Schlender P, Kleinke H. Thermoelectric properties of $Tl_{10-x}Ln_xTe_6$, with Ln = Ce, Pr, Nd, Sm, Gd, Tb, Dy, Ho and Er, and $0.25 \leq x \leq 1.32$. *Journal of Alloys and Compounds*. 2013;549:126-134.

26. Bangarigadu-Sanasy S, Sankar CR, Dube PA, Greedan JE, Kleinke H. Magnetic properties of Tl_9LnTe_6, Ln = Ce, Pr, Tb and Sm. *Journal of Alloys and Compounds*. 2014;589:389-392.

27. Guo Q, Kleinke H. Thermoelectric properties of hot-pressed Tl_9LnTe_6 (Ln = La, Ce, Pr, Nd, Sm, Gd, Tb) and $Tl_{10-x}La_xTe_6$ ($0.90 \leq x \leq 1.05$). *Journal of Alloys and Compounds*. 2015;630:37-42.

28. Andreev OV, Bamburov VG, Monina LN, Razumkova IA, Ruseikina AV, Mitroshin OY, Andreev VO. *Phase equilibria in the sulfide systems of the 3d, 4f-elements*. Ekaterinburg: Editorial Publication Department of the UR RAS; 2015.

29. Tomashik V, Feychuk P, Shcherbak L. *Ternary Alloys Based on II-VI Semiconductor Compounds*. Chernivtsi: Books-XX1; 2010.

30. Babanly MB, Chulkov EV, Aliev ZS, Shevelkov AV, Amiraslanov IR. Phase diagrams in materials science of topological insulators based on metal chalkogenides. *Russian Journal of Inorganic Chemistry*. 2017;62(13):1703-1729.

31. Ioffe AF. *Semiconductor Thermoelements and Thermoelectric Cooling*. London: Infosearch Limited; 1957.

32. Imamaliyeva SZ, Gasanly TM, Gasymov VA, Babanly MB. Phase Equilibria and some Properties of Solid Solutions in the Tl_5Te_3-Tl_9SbTe_6-Tl_9GdTe_6 System. *Acta Chimica Slovenia*. 2017;64(1):221-226.

33. Imamaliyeva SZ, Gasanly TM, Zlomanov VP, Babanly MB. Phase Equilibria in the Tl_5Te_3-Tl_9BiTe_6-Tl_9TbTe_6 system. *Inorganic Materials*. 2017;53(7):685-689.

34. Imamaliyeva SZ, Firudin MI, Gasymov VA, Babanly MB. Phase equilibria in the Tl_5Te_3-Tl_9BiTe_6-Tl_9TmTe_6 section of the Tl-Bi-Tm-Te Quaternary System. *Materials Research*. 2017;20(4):1057-1062.

35. Imamaliyeva SZ, Hasanly TM, Gasymov VA, Babanly MB, Sadygov FM. Phase relations in the Tl_9GdTe_6-Tl_9SbTe_6 and Tl_9TbTe_6-Tl_9SbTe_6 systems. *Chemical Problems*. 2017;3:241-247.

36. Bradtmöller S, Böttcher PZ. Darstellung und Kristallstruktur von $SnTl_4Te_3$ und $PbTl_4Te_3$. *Zeitschrift für anorganische und allgemeine Chemie*. 1993;619(7):1155-1160.

37. Doert T, Böttcher P. Crystal structure of bismuthnonathallium hexatelluride $BiTl_9Te_6$. *Zeitschrift für Kristallographie*. 1994;209:95.

38. Babanly MB, Dashdiyeva GB, Huseynov FN. Phase equilibriums in the Tl_4PbTe_3-Tl_9BiTe_6 system. *Chemical Problems*. 2008;1:69-72.

39. Glazov VM, Vigdorovich VN. *Mikrotverdost' metallov i poluprovodnikov*. Moscow: Metallurgiya; 1969. (In Russian).

40. Ferey G. *Crystal Chemistry. From Basics to Tools for Materials Creation*. New Jersey: World Scientific; 2017.